Stereospecific Differences in Repair by Human Cell Extracts of Synthesized Oligonucleotides Containing trans-Opened 7,8,9,10-Tetrahydrobenzo[*a*]pyrene 7,8-Diol 9,10-Epoxide N^2-dG Adduct Stereoisomers Located within the Human K-*ras* Codon 12 Sequence†

Laura Custer,‡,§,|| Barbara Zajc,⊥ Jane M. Sayer,⊥ Carleen Cullinane,# Don R. Phillips,# Albert M. Cheh,||,⊥ Donald M. Jerina,⊥ Vilhelm A. Bohr,‡ and Sharlyn J. Mazur*,‡

Laboratory of Molecular Genetics, National Institute on Aging, The National Institutes of Health, Baltimore, Maryland 21224-6825, Laboratory of Bioorganic Chemistry, National Institute of Diabetes and Digestive and Kidney Diseases, The National Institutes of Health, Bethesda, Maryland 20892-0820, School of Biochemistry, LaTrobe University, Bundoora, Victoria, Australia 3083, and Department of Chemistry, American University, Washington D.C. 20016-8014

Received June 5, 1998; Revised Manuscript Received September 30, 1998

ABSTRACT: The potent environmental carcinogen benzo[*a*]pyrene (BaP), following enzymatic activation to enantiomeric pairs of bay-region 7,8-diol 9,10-epoxides (the benzylic 7-hydroxyl group and epoxide oxygen are cis for DE-1 diastereomers and trans for DE-2 diastereomers), reacts with DNA to form covalent adducts predominately at the exocyclic amino groups of purines. Specific adducts, corresponding to the trans opening of each of the four optically active BaP DE isomers at C-10 by the N^2-amino group of dG, were synthesized as appropriately blocked phosphoramidites and were incorporated at either the first or second G of codon 12 within the G-rich sequence of human K-*ras* codons 11−13: GCT G_1G_2T GGC. The adducted oligonucleotides were incorporated into plasmids by primer extension, followed by purification of the covalently closed circular constructs. Adducts derived from either (+)- or (−)-DE-2, placed at either G_1 or G_2, presented strong blocks to in vitro transcription elongation by bacteriophage T3 RNA polymerase, but only moderately blocked transcription elongation by human RNA polymerase II in nuclear extracts. Adducts derived from all four DEs, placed on either G_1 or G_2, were used as substrates in a DNA repair synthesis assay using human whole cell extracts. Adducts derived from three of the DE stereoisomers exhibited significant amounts of repair synthesis, but the (−)-DE-2 adduct experienced no repair synthesis above that of the control. Constructs containing a pre-existing nick at the sixth phosphodiester bond 3′ to either (+)-DE-2 or (−)-DE-2 adducts exhibited increased repair synthesis.

Chemical carcinogenesis is a complex multistage process (*1*) requiring mutations in multiple crucial genes. DNA repair is of critical importance because DNA damages that are not repaired can become expressed as mutations. As part of their normal excretory process, animals metabolize nonpolar xenobiotic chemicals into more hydrophilic species, which are more easily eliminated (*2*). Oxidative metabolism of the environmentally ubiquitous polycyclic aromatic hydrocarbons (PAH)[1] generates chemically reactive arene oxides and benzo-ring diol epoxides (*3*). Bay-region diol epoxides (DEs) have been established as ultimate carcinogens of the PAHs (*4*−*6*). Specifically, the potent environmental carcinogen benzo[*a*]pyrene (BaP) is metabolized to a diastereomeric pair of 7,8-diol 9,10-epoxides in which the benzylic 7-hydroxyl group and epoxide oxygen are either cis (DE-1) or trans (DE-2) as shown in Figure 1. The combined stereoselectivity of cytochrome P450 and epoxide hydrolase results in the formation of (+)-DE-2 as the major stereoisomer in liver (*7*). Interestingly, this same stereoisomer is the only one of the set of four optically active DEs that has high tumorigenic activity (*6*, *8*). The primary targets for covalent modification of DNA by the DEs are the exocyclic amino groups of the purine bases (*9*). In the case of the BaP DEs, particularly (+)-DE-2, binding to dG is favored over dA (*10*, *11*). The trans-ring-opened dG products of the BaP DE isomers are also shown in Figure 1.

† This research was supported, in part, by a fellowship to L.C. from the U.S. Department of Education and the Department of Chemistry, American University.

* To whom correspondence should be addressed.

‡ NIA, NIH.

§ Present address: Genetic Toxicology, Covance Laboratories Inc., Vienna VA.

|| American University.

⊥ NIDDK, NIH.

LaTrobe University.

[1] Abbreviations: PAH, polycyclic aromatic hydrocarbon; BaP, benzo[*a*]pyrene; DE, diol epoxide (DE-1 in which the benzylic 7-hydroxyl and epoxide oxygen are cis and DE-2 in which these groups are trans); (+)-BaP DE-2 or (+)-DE-2, (7*R*,8*S*,9*S*,10*R*)-7,8-dihydroxy-9,10-epoxy-7,8,9,10-tetrahydrobenzo[*a*]pyrene; (−)-BaP DE-2 or (−)-DE-2, the (7*S*,8*R*,9*R*,10*S*)-enantiomer; (+)-BaP DE-1 or (+)-DE-1, (7*S*,8*R*,9*S*,10*R*)-7,8-dihydroxy-9,10-epoxy-7,8,9,10-tetrahydrobenzo[*a*]-pyrene; (−)-BaP DE-1 or (−)-DE-1, the (7*R*,8*S*,9*R*,10*S*)-enantiomer; DMT, dimethoxytrityl; di-*O*-TBDMS-2-FdI, 3′,5′-di-*O*-(*tert*-butyldi-methylsilyl)-2-fluoro-2′-deoxyinosine; CPG, controlled pore glass; CD, circular dichroism; NER, nucleotide excision repair; TCR, transcription coupled repair; AdML, adenoviral major late (promoter); T4 PNK, phage T4 polynucleotide kinase; WCE, whole cell extract.

10.1021/bi9813330 CCC: $18.00
Published on Web 12/19/1998

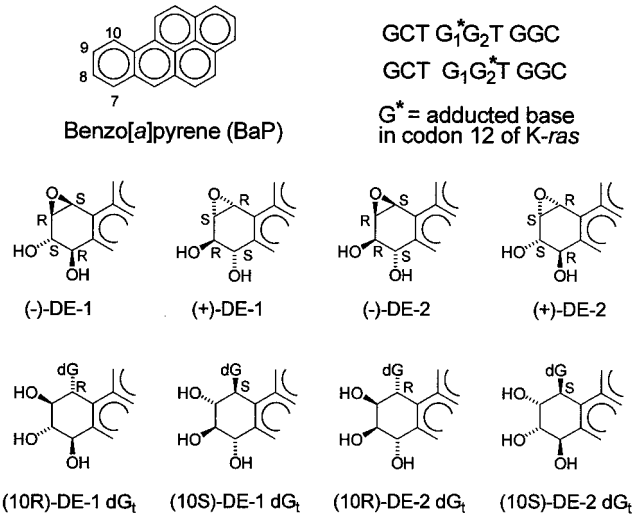

FIGURE 1: Benzo[*a*]pyrene, its diol epoxide stereoisomers and their trans-ring-opened products, and the DNA 9-mers encompassing codons 11−13 of the human K-*ras* gene. Adducts were placed on G_1 or G_2 of codon 12.

The conformation of BaP DE adducts in double-stranded DNA is determined predominantly by DE stereochemistry and whether the purine is A or G. Solution conformations of oligonucleotide duplexes containing BaP DE adducts have been studied by 2D NMR (*12, 13*) as well as by absorbance and fluorescence spectroscopy (*14, 15*). For trans-opened adducts at dA, the hydrocarbon is intercalated toward the 3′-end of the adducted strand for the 10*S* adduct (16) and the 5′-end for the 10*R* adduct (*17*). For trans-opened adducts at dG, the hydrocarbon is groove-bound and lies toward the 3′-end of the adducted strand for the 10*R* adduct and the 5′-end for the 10*S* adduct (*18, 19*). Adducts at dG formed by cis ring opening of (+)- or (−)-DE-2 are intercalated into the helix with displacement of the modified G into the minor or major grooves, respectively (*20, 21*). Although most of the NMR data have been collected for structures with dC flanking the adducted base, some evidence suggests that changing the identity of the 5′-flanking base may lead to conformational heterogeneity (*22, 23*). Detailed structural studies of the DE-1 dG adducts are not yet available.

DNA targets of particular interest are tumor suppressor genes, such as p53, or proto-oncogenes, such as *ras*. The *ras* family of genes, members of which are frequently mutated in certain types of cancer (*24, 25*), is involved in controlling cell proliferation in response to external signals (*26*). Mutation at any of the four Gs within codons 12 or 13 leads to activation of the *ras* oncogene protein. Mutation hotspots within these genes are often preferential targets for BaP DE adduct formation (*27, 28*).

The cellular response to BaP DE adduct formation includes DNA repair to prevent the fixation of damage into mutations. Bulky adducts, such as those produced by BaP DEs, are removed by the nucleotide excision repair (NER) system. The characteristics of the mammalian NER system are best understood for the repair of pyrimidine dimers induced by ultraviolet (UV) radiation. Cyclobutane pyrimidine dimers are removed more rapidly in actively transcribed genes than from the genome as a whole (*29*), and in particular are removed from the transcribed strand of RNA polymerase II-transcribed DNA more rapidly than from the nontranscribed strand (*30, 31*). The sequence context of the lesion also influences the rate of repair, with sites of slow repair frequently corresponding to mutation hot spots (*32, 33*). A similar pattern of preferential repair of BaP DE adducts is suggested by the preponderance of mutations at sites of purines in the nontranscribed strand in both hamster and human cells (*34*−*36*). DNA damage produced by BaP DE is removed more rapidly from the transcribed than nontranscribed strand of an actively transcribed gene in human fibroblasts (*37*), but in hamster cells the damage is removed from active genes at the same rate as from the overall genome (*38*). The damage produced by a related compound, benzo[*c*]phenanthrene diol epoxide, is preferentially repaired in the transcribed strand of active genes in hamster cells (*39*).

Most studies to date of the characteristics of stereochemically defined BaP DE adducts have focused on adducted purines flanked by pyrimidines. In this paper we have synthesized oligonucleotide 9-mers containing trans-opened dG adducts of each of the four individual BaP DE stereoisomers (Figure 1) placed at either the first G or the second G of codon 12 in the G-rich sequence of human K-*ras*. We have incorporated these oligonucleotides into covalently closed circular plasmids and have examined the effect of the adducts on transcription elongation by purified bacteriophage T3 RNA polymerase or by human RNA polymerase II in nuclear extracts. We have examined the repair of these adducts by human whole cell extracts using an in vitro DNA repair synthesis assay.

MATERIALS AND METHODS

Unmodified Oligonucleotides. The unmodified 9-mer (GCTGGTGGC), the 5′-flanking 23-mer (5′-GCTCTAGAACTAGTGGATCCCCC, as the 5′-phosphate) and the 3′-flanking 16-mer (GGCTGCAGGAATTCG) used in construction of single-lesion plasmids and nicked constructs were obtained from Operon Technologies. The 3′-flanking 16-mer was purified by HPLC. The unmodified 9-mer and the 5′-flanking 23-mer were purified by electrophoresis through an 18% polyacrylamide gel followed by passage through a C18 Sep-pak (Waters) (*40*).

Synthesis of Oligonucleotides Containing Trans-Opened BaP Diol Epoxides Covalently Bound to the Exocyclic Amino Group of Deoxyguanosine. Adduct Formation. The aminotriols derived from trans opening of racemic BaP DE-1 (*41*) or DE-2 (*42*) at C-10 were prepared by ammonolysis of the corresponding diol epoxides (*43*). These were allowed to react with a 1.5-fold molar excess of 3′,5′-di-*O*-(*tert*-butyldimethylsilyl)-2-fluoro-2′-deoxyinosine (di-*O*-TBDMS-2-FdI) (*44*) (see Scheme 1) in Me_2SO and hexamethyldisiloxane containing 2,6-lutidine with heating for 3 h (DE-1 aminotriol) or 4.5 h (DE-2 aminotriol). A typical reaction mixture contained 60 mg of aminotriol and 140 mg of 2-di-*O*-TBDMS-2-FdI in 1.4 mL of Me_2SO, 5.8 mL of hexamethyldisiloxane and 41 μL of 2,6-lutidine. Disappearance of the starting aminotriol (T_R =11−13 min) was monitored by reversed-phase HPLC on a Beckman Ultrasphere C_{18} column (5 μm, 4.6 × 250 mm), eluted at 1.5 mL/min with a gradient that was ramped from 60% 0.01 M NH_4OAc (pH 7)/40% MeOH to 100% MeOH in 20 min and maintained at 100% MeOH for 5 min. The reaction mixture was cooled to room temperature, diluted with ethyl acetate, and washed

Scheme 1

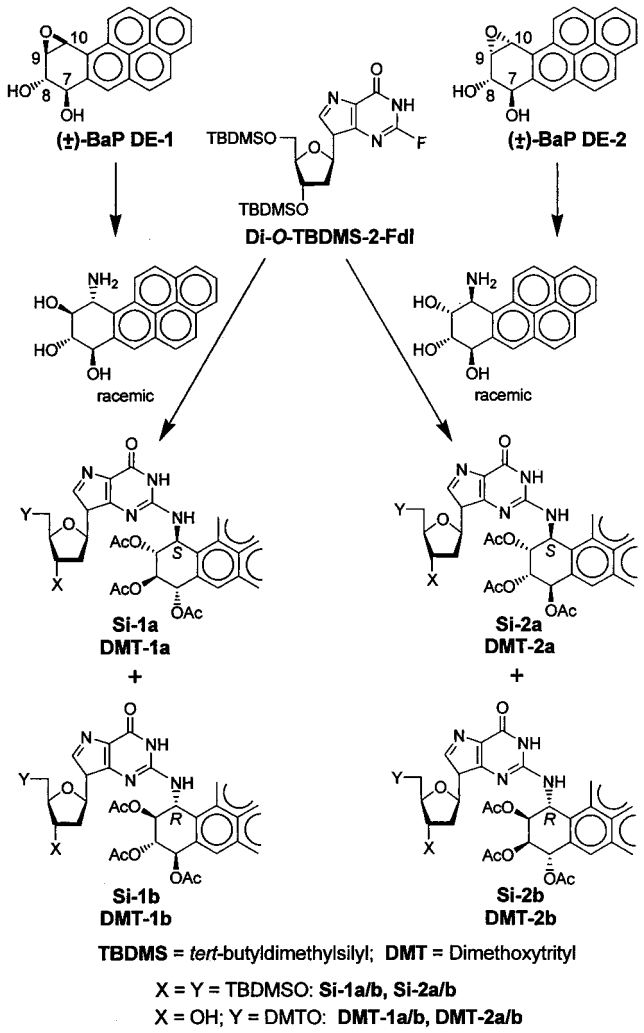

with brine. The aqueous layer was extracted three times with ethyl acetate, and the combined ethyl acetate extracts were dried (Na_2SO_4) and evaporated under reduced pressure. The crude product thus obtained was acetylated without purification, by reaction with acetic anhydride/pyridine (1:1) for 15 h. After solvent evaporation the mixture of diastereomers was purified by preparative TLC (SiO_2, CH_2Cl_2 50%, C_6H_6 40%, MeOH 10%, developed twice for DE-1 products; EtOAc 60%, CH_2Cl_2 30%, MeOH 10% for DE-2 products). Diastereomeric pairs of adducts in both the DE-1 and DE-2 series separate on HPLC (Axxiom silica column, 5 μm, 10 $\times$ 250 mm; conditions given in the Supporting Information). Previous studies on guanosine (*11*, *45*) and deoxyguanosine (*10*) adducts derived from attack of the 2-amino group of guanine nucleotides on optically active diol epoxides had established a correlation between circular dichroism (CD) spectra and absolute configuration such that a strong positive band at ~250 nm was indicative of 10*S*, and a strong negative band was indicative of 10*R* configuration at the site of attachment of the amino group to the hydrocarbon. CD spectra of the diastereomeric pairs of adducts **Si-1a** and **Si-1b**, **Si-2a** and **Si-2b** (see Scheme 1 for structures), were essentially identical in shape to those previously reported for the unprotected guanosine derivatives derived from trans opening of DE-1 (*45*) and deoxyguanosine derivatives from DE-2 (*10*). The less-polar isomers (**Si-1a** and **Si-2a**, see Scheme 1) in both the DE-1 and DE-2 series were assigned 10*S* absolute configuration on the basis of positive bands in their CD spectra (MeOH): **Si-1a**, $\Delta\epsilon$ 64 (249 nm); **Si-2a**, $\Delta\epsilon$ 103 (250 nm). Similarly, the more polar isomers (**Si-1b** and **Si-2b**) exhibited negative CD bands at this wavelength, indicative of 10*R* configuration: **Si-1b**, $\Delta\epsilon$ −81 (249 nm); **Si-2b**, $\Delta\epsilon$ −112 (249 nm). NMR and mass spectra are given in the Supporting Information. Yields of the diastereomeric pairs of acetylated adducts **Si-1a/b** and **Si-2a/b** were 61% and 37%, respectively, for the two steps from aminotriol.

Desilylation of the Sugar Hydroxyl Groups. The mixed diastereomers in the DE-1 (**Si-1a/b**) and DE-2 series (**Si-2a/b**) were treated with a 1:1 mixture of 20% HF/pyridine (*46*) and dry CH_3CN at room temperature for 3 h (DE-1 series) or 5 h (DE-2 series). After dilution with EtOAc and standard workup, the crude products as mixed diastereomers were obtained in quantitative yield. FAB HRMS: calculated for $C_{36}H_{33}O_{10}N_5$ *m/z* 695.2227, found 695.2313 (DE-1 series), found 695.2239 (DE-2 series) (M^+). Separated diastereomers **Si-2a** and **Si-2b** were desilylated to yield the corresponding individual diastereomers with free sugar hydroxyl groups by the same procedure. Product from **Si-2a** was obtained in 95% yield after purification by TLC (SiO_2, CH_2Cl_2 70%, *n*-hexane 20%, MeOH 10%, developed twice). FAB HRMS: calculated for $C_{36}H_{34}O_{10}N_5$ *m/z* 696.2306, found 696.2322 ($M+1^+$). Product from **Si-2b** was obtained in 86% yield after purification by HPLC (Axxiom silica column, 5 μm, 10 $\times$ 250 mm, CH_2Cl_2 70%, *n*-hexane 22%, MeOH 8%, flow rate 5 mL/min). FAB HRMS: calcd for $C_{36}H_{34}O_{10}N_5$ *m/z* 696.2306, found 696.2291 ($M+1^+$).

Preparation of 5′-O-Dimethoxytrityl Derivatives. The above desilylated triacetates were treated at room temperature with DMT tetrafluoroborate (*47*) in 2,6-lutidine (4−5 mL/mg of triacetate) containing a 2-fold molar excess of Li_2CO_3. The pair of diastereomers in the DE-1 series was allowed to react for 3 h with a 10% molar excess of the tetrafluoroborate, followed by extraction into ethyl acetate, standard workup, and purification by preparative TLC (SiO_2, CH_2Cl_2 91%, MeOH 8%, NEt_3 1%; 76% yield of the diastereomer mixture). The pair of diastereomeric DMT derivatives could be separated by TLC (SiO_2, CH_2Cl_2 91%, i-PrOH 8%, NEt_3 1%). The less-polar (faster-migrating) diastereomer was assigned 10S absolute configuration (**DMT-1a**) on the basis (see above) of its CD spectrum, which exhibited a strong, positive band at 249 nm. The individual diastereomers (**Si-2a** and **Si-2b**) of the desilylated triacetates in the DE-2 series were allowed to react for a total of 4.5 h with a 1.5-fold molar excess of the DMT tetrafluoroborate, added in two portions. After extraction with CH_2Cl_2 and standard workup each product was purified by TLC. **DMT-2a**, derived from **Si-2a**, was isolated in 79% yield after TLC (SiO_2, CH_2Cl_2 79%, EtOAc 15%, MeOH 5%, NEt_3 1%). **DMT-2b**, derived from **Si-2b**, was isolated in 70% yield after TLC (SiO_2, CH_2Cl_2 70%, *n*-hexane 20%, MeOH 9%, NEt_3 1%). NMR and mass spectra are given in the Supporting Information.

3′-[2-Cyanoethyl-N,N-Diisopropyl]phosphoramidites. These were prepared from the individual diastereomers **DMT-2a** and **DMT-2b** and from the diastereomer mixtures **DMT-1a/b** and **DMT-2a/b** by reaction with 2-cyanoethyl-*N*,*N*-diisopropylchlorophosphoramidite (*48*). The following procedure is typical. A mixture of DMT-protected diastereo-

mers (34 mg, 35 μmol) was stirred in dry methylene chloride (0.6 mL). EtN(i-Pr)$_2$ (30 μL) was added, the reaction mixture was cooled to −30 °C, and 2-(cyanoethyl)-*N*,*N*-diisopropylchlorophosphoramidite (9.4 μL, 42 μmol) was added under argon. The reaction mixture was stirred at 0−5 °C for 45 min, another 9.4 μL of 2-(cyanoethyl)-*N*,*N*-diisopropylchlorophosphoramidite was added at −30 °C, and stirring was continued at 0−5 °C for another 15 min. Products were extracted into methylene chloride and dried over sodium sulfate. After solvent concentration in vacuo, the products were purified by preparative TLC: Products from **DE-1** series (80%) (SiO_2, CH_2Cl_2 96%, MeOH 3%, EtN(i-Pr)$_2$ 1%). ^{31}P NMR ($CDCl_3$, 0.1 M H_3PO_4 external standard): 149.51 (broad s). Products from **DE-2** series (73%) (SiO_2, CH_2Cl_2 81%, EtOAc 15%, MeOH 3%, NEt_3 1%, developed twice). ^{31}P NMR ($CDCl_3$, 0.1 M H_3PO_4 external standard): 149.41 (broad s).

Oligonucleotide Syntheses from Phosphoramidites. With the exception of the two oligonucleotides GCT G_1G_2*T GGC with a central, modified deoxyguanosine (G*) corresponding to the adduct formed by trans addition of the 2-amino group of dG to (+)- and (−)-BaP DE-1 (see below), modified oligonucleotides were synthesized by use of the adducted phosphoramidites prepared as described in the preceding section. The oligonucleotide GCT G_1G_2*T GGC containing BaP DE-2 adducts on the second G of *ras* codon 12 was prepared stereospecifically from separated phosphoramidites with 10*R* and 10*S* absolute configuration; for oligomers containing adducts on the first G (GCT G_1*G_2T GGC), a mixture of diastereomeric phosphoramidites was used. Syntheses were carried out on a 2−10 μmol scale using an Applied Biosystems Model 392 synthesizer to generate the sequence 3′ to the modified nucleoside, with a manual step for coupling of the adducted phosphoramidite, as previously described (*42*, *47*). A typical 2-μmol synthesis utilized 21 mg of benzoyl dC substituted controlled pore glass (CPG) (170 Å, 95 μmol/g), with addition of 4.5 mg (3.75 μmol) of the appropriate dG-adducted phosphoramidite and 60 μL of 0.5 M tetrazole (CH_3CN solution) in the manual coupling step. Coupling was allowed to proceed for 17−22 h, at the end of which time the synthesis was completed automatically. Efficiency of the manual coupling step, as measured by spectrophotometric (496 nm) assay of DMT cation released upon detritylation of the coupling product, was typically 20−30% for syntheses using the high-load CPG support. End-capping by acetylation, which ordinarily facilitates purification of products as their DMT derivatives by preventing unreacted oligonucleotide chains from undergoing elongation in subsequent cycles, was found to be unnecessary after the manual step, since the hydrocarbon is sufficiently hydrophobic to permit easy separation of full-length, adducted oligonucleotides from deletion sequences lacking the hydrocarbon that result from elongation of chains that failed to couple with the adducted phosphoramidite. Thus, end-capping was omitted after the manual step in the synthesis of the four oligonucleotides 5′-GCT G_1*G_2T GGC-3′ (where G* represents either a DE-1 or DE-2 adduct), to avoid termination of chains that might have lost the 5′-DMT group during extended coupling times.

Oligonucleotide Syntheses by Postoligomerization Modification. The pair of oligonucleotides, GCT G_1G_2*T GGC with a central, modified deoxyguanosine (G*) corresponding to the adduct formed by trans addition of the 2-amino group of dG to (+)- and (−)-BaP DE-1, were prepared by the method of postoligomerization modification (*49*). The requisite CPG-bound 9-mer (82 mg, 4 μmol) containing a central 2-fluorodeoxyinosine residue was allowed to react (55−58 °C, 5 days) with the aminotriol derived from (±)-BaP DE-1 (20 mg, 63 μmol) in a mixture of Me_2SO (1.4 mL), hexamethyldisiloxane (5.8 mL), and 2,6-lutidine (41 μL). Preparation of CPG-bound oligonucleotides containing a 2-fluorodeoxyinosine residue as well as details of the workup of postoligomerization modification products from BaP aminotriols have been described elsewhere (*41*, *50*).

Purification and Characterizaton of the Adducted 9-mers. The BaP diol epoxide-modified oligonucleotides were purified by reversed-phase HPLC as their 5′-DMT derivatives, detritylated (80% HOAc in H_2O), and subjected to a second reversed-phase HPLC purification. The latter resolved pairs of oligomers produced from diastereomeric phosphoramidites or by postoligomerization modification. For HPLC conditions and retention times, see Supporting Information. The presence of the BaP DE adducts on the 9-mers was also demonstrated by gel mobility differences. The adducted 9-mers and the undamaged control were end-labeled with [α-^{32}P]-ATP and bacteriophage T4 polynucleotide kinase (Epicentre Technologies) using the manufacturer's suggested conditions. Nucleotides used in the labeling were removed by ultrafiltration. Samples were separated by electrophoresis through a denaturing 12% polyacrylamide gel. The dried gel was exposed to a PhosphoImager 400E screen.

Construction of the Vector. The phagemid pKS(+)Ad-*ras*12, which contains the adenovirus major late promoter and nine bases of the human *ras* sequence from codons 11−13 (Figure 2), was constructed by the following steps. A 9-base pair (bp) insert containing the sequence of the human K-*ras* codons 11−13 was cloned into the *Sma*I site of phagemid pBluescript II KS(+) (Stratagene) oriented such that the sequence 5′-GCTGGTGGC-3′ was placed into the (−) strand. The presence and orientation of the *ras* insert was confirmed by Southern blot and sequencing. The resulting pKS(+)*ras*12 plasmid was digested with *Kpn*I and *Hinc*II, removing a 19-bp fragment. A 70-bp fragment containing the Adenovirus major late (AdML) promoter (*51*)- was ligated to the complementary ends, generating the vector pKS(+)Ad-*ras*12. Upon construction of the single-lesion plasmids, the adducts located on G_1 of the *ras* codon 12 sequence are located in the transcribed strand, 64 and 135 nucleotides downstream of the AdML and T3 promoters, respectively. Note that the sequence of the K-*ras* codons 11−13 corresponds to the coding (nontranscribed) strand of the human gene.

Single-Stranded pKS(+)Ad-ras Preparation. The double-stranded phagemid pKS(+)Ad-*ras* was transformed into competent DH11S cells (Life Technologies). Phage were produced following infection with M13KO7 helper phage (*40*). After overnight incubation, bacteria were removed by centrifugation. Phage were collected by PEG-NaCl precipitation (*40*). DNA was recovered from the phage by digestion at a concentration of 100−200 μg/mL with 500 μg/mL proteinase K in 10 mM Tris-HCl (pH 8.0), 2.5 mM EDTA, and 0.25% SDS for 1 h at 42 °C. DNA was precipitated by addition of NaCl and ethanol, recovered by centrifugation, and dissolved in 1−2 mL of TE. Single-stranded DNA circles

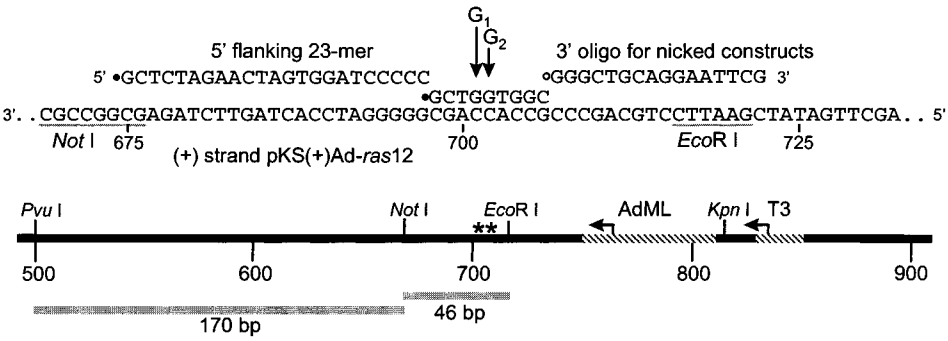

FIGURE 2: Construction of plasmids containing single stereospecific benzo[*a*]pyrene diol epoxide adducts. The 9-mer annealing around position 700 of pKS(+)Ad-*ras*12 contains the sequence of the human K-*ras* codons 11−13 and a BaP adduct placed on either G_1 or G_2. The 5′-flanking 23-mer was ligated to the 9-mer to produce a stable primer for second strand synthesis. The nonphosphorylated 3′-oligomer was used in making the nicked constructs. The adducts are located in the transcribed strand with respect to the adenovirus major late promoter (AdML) and the T3 promoter, indicated by hatching, although the *ras* sequence corresponds to the coding (nontranscribed) strand in the intact gene. The fragments used for the analysis of DNA repair are represented by gray bars. The repair patch produced by nucleotide excision repair is entirely located within the 46-bp *Eco*RI−*Not*I fragment. The 170-bp *Not*I−*Pvu*I fragment was used to correct for nonspecific DNA repair synthesis.

were purified by equilibrium centrifugation in a CsCl solution of density 1.70 g/mL in a VTi65.2 rotor at 40 000 rpm for 16 h at 25 °C. Fractions containing the DNA were pooled and desalted using a Centricon-30 filtration unit.

Test of Efficiency of 9-mer Annealing and Ligation. The 9-mers containing the BaP DE adducts do not anneal with sufficient stability to the single-stranded circles to be used as primers in the primer extension method of single-lesion plasmid construction. A 23-base oligonucleotide lying just 5′ to the adducted oligonucleotide was used to create a stable primer (Figure 2). A test was performed to determine the efficiency of annealing and ligation of the adducted 9-mers to the 5′-flanking oligomer. Twenty picomoles of the 5′-flanking 23-mer was annealed to single-stranded pKS(+)-Ad-*ras* followed by addition of radioactively labeled, adducted 9-mer at a 1:1:10 mole ratio in 100 μL of reaction mix containing 50 mM Tris-HCl, (pH 8), 20 mM KCl, 7 mM $MgCl_2$, and 0.1 mM EDTA. The tube was incubated at 70 °C for 5 min and allowed to cool slowly to 37 °C. Ligation was performed in 16 μL by adding 1 μL of 100 mM ATP, 4 μL of sterile water, and 1 μL of T4 DNA ligase diluted to 0.4 units/μL, to 10 μL of the annealing mix and incubating overnight at 16 °C. Nucleotides and unannealed oligomers were removed by ultrafiltration. The recovered DNA was examined by electrophoresis through a denaturing 8% polyacrylamide gel. After soaking in water and drying, the gel was transferred to a PhosphoImager 400E cassette and allowed to expose for 2 days before analysis.

Single-Lesion Plasmid Construction. Single-stranded DNA circles and 5′-flanking 23-mer were annealed in a 250 μL reaction mix containing 50 pmol of single-stranded DNA circles and 50 pmol of phosphorylated 23-mer in a buffer of 50 mM Tris-HCl (pH 8.0), 20 mM KCl, 7 mM $MgCl_2$, 0.1 mM EDTA. Samples were incubated at 70 °C for 5 min and then allowed to cool slowly to 37 °C. Annealed samples were transferred to tubes containing a 10-fold molar excess (500 pmol) of dried, phosphorylated 9-mer bearing a specific BaP DE adduct. After addition of ATP to 1 mM and 10 units of T4 DNA ligase, the tubes were incubated overnight at 16 °C. Reactions were assembled on ice. Primer extension was performed in a solution containing 33 mM Tris-HCl (pH 8.8), 66 mM potassium acetate, 10 mM magnesium acetate, 0.5 mM DTT, 500 μM each of dGTP, dCTP, dATP, and dTTP, 0.2 mM ATP, 100 μg of T4 gene 32 protein, 50 units of T4 DNA ligase, and 50 units of T4 DNA polymerase in a volume of 500 μL. The tubes were incubated on ice for 5 min and then placed at room temperature for 10 min, followed by incubation at 37 °C for 1.5 h. The single-lesion closed circular duplex constructs were purified by two sequential CsCl/ethidium bromide gradients. Ethidium bromide was removed by butanol extraction, and the samples were desalted with a Centricon 30 unit. The content of nicked circles in the purified covalently closed circular constructs was determined by gel electrophoresis, taking into account the difference in ethidium bromide binding between the nicked and the moderately supercoiled constructs. Single-lesion constructs prepared in this manner have a low superhelical density and consequently bind 2.4-fold less ethidium bromide than linear DNA.

Nicked Circular Constructs. Duplex constructs containing a nick specifically located at the sixth phosphodiester bond 3′ to the adducted base were produced for adducts derived from BaP (+)-DE-2 and (−)-DE-2 on G_1. The corresponding undamaged nicked construct was produced as well. The nicked constructs were prepared by the procedure described above with the addition of a nonphosphorylated oligonucleotide annealed 3′ to the adducted oligonucleotide. Single-stranded pKS(+)Ad-*ras*12 DNA, the phosphorylated 5′-flanking 23-mer, the adducted phosphorylated 9-mer, and a nonphosphorylated 3′-flanking 16-mer were annealed in a 1:1:10:1 mole ratio. The reaction conditions for phosphorylation, annealing, ligation, and extension were identical to those described above. The 9-mer and 5′-flanking 23-mer were ligated to produce a 32-base oligonucleotide containing the damage. Primer extension from the annealed 3′-flanking oligomer was followed by ligation to produce a double-stranded construct with a nick at the sixth phosphodiester bond 3′ to the adducted base. The constructs were purified by two sequential CsCl/ethidium bromide gradients.

Cell Culturing and Extracts. Transformed lymphoblasts (GM01310b) from an apparently normal donor were obtained from the Coriell Human Genetic Mutant Cell Repository. Cells were cultured in RPMI 1640 supplemented with 13% fetal bovine serum (FBS), 2 mM L-glutamine, 100 units/mL penicillin G, and 100 μg/mL streptomycin sulfate. Whole cell extracts (WCE) were prepared as described (*52*). The

WCE exhibited the expected proficiency in damage-specific DNA repair synthesis on undamaged and AAAF-damaged plasmids (*53*). HeLa cells were cultured in RPMI 1640 supplemented with 10% FBS, 2 mM L-glutamine, 100 units/mL penicillin G, and 100 μg/mL streptomycin sulfate. Nuclear extracts were prepared essentially as described (*54*).

Blockage of Bacteriophage T3 Transcription. Single-lesion plasmids were linearized by reaction with Turbo *Nae*I (Promega). The linear product was incubated in a buffer containing 40 mM Tris-HCl (pH 7.9), 6 mM $MgCl_2$, 2 mM spermidine, 10 mM NaCl, 10 mM DTT, 0.5 mM each of ATP, CTP, and GTP, 50 μM UTP, and 10 μCi [α-^{32}P]-UTP (3000 Ci/mmol) in a volume of 20 μL. Reactions were initiated by addition of 5 units of T3 RNA polymerase and were incubated at 37 °C for 5 or 10 min. Reactions were terminated by addition of formamide loading buffer. Reaction products were separated on a denaturing 6% polyacrylamide gel. The gel was fixed and dried. The incorporated radioactivity was visualized using a PhosphorImager (Molecular Dynamics). The degree of lesion bypass was determined from the radioactivity incorporated into the blocked transcripts (132−134 bases) and full-length transcript (505 bases), taking into account that the blocked transcript contains 29 uracils and the full-length transcript contains 109 uracils.

Blockage of RNA Polymerase II Transcription. Constructs were linearized with *Nae*I. Linear products at 50 nM were incubated in a buffer containing 37.5 mM Hepes-KOH (pH 7.9), 70 mM KCl, 8.5 mM $MgCl_2$, 1.5 mM DTT, 0.5 mM EDTA, 8.5% glycerol, 0.4 units/μL RNase inhibitor, 500 μM each of ATP, CTP, and GTP, 10 μM UTP, 10 μCi [α-^{32}P]-UTP, and 70 μg of nuclear extract protein in a volume of 40 μL. Samples were incubated at 30 °C for up to 90 min. The samples were then adjusted to 0.2 mg/mL Proteinase K and 0.4% SDS and incubated at 30 °C for a further 30 min before being extracted once with phenol and once with chloroform and ethanol precipitated. The pellets were rinsed with 70% ethanol, dried, and resuspended in formamide loading dye. The samples were denatured, and the products were separated on a 6% denaturing polyacrylamide gel and processed as described above. The adducts are located at positions 63 and 64 from the start of transcription for the G_1G_2*T and G_1*G_2T constructs, respectively. The full-length transcript is 434 bases. The transcript up to the position of the adducts contains 17 uracils, and the full-length transcript contains 97 uracils.

In Vitro DNA Repair Synthesis Assay. DNA repair synthesis assays were based on established procedures (*52*). Briefly, 200 ng of single-lesion plasmid and 100 μg of WCE protein were combined in a solution containing 45 mM HEPES−KOH (pH 7.8), 70 mM KCl, 7.5 mM $MgCl_2$, 0.5 mM EDTA, 1.25 mM DTT, 3.4% glycerol, 12.5 μg of BSA, 5 μg of creatine phosphokinase, 50 mM phosphocreatine, 2 mM ATP, 50 μM each of dATP, dGTP, and dTTP, 5 μM dCTP, and 1 μCi [α-^{32}P]-dCTP (3000 Ci/mmol) in a final volume of 50 μL. All components except DNA were mixed and incubated at 30 °C for 5 min, followed by addition of DNA and further incubation at 30 °C for up to 90 min. The reactions were stopped by addition of EDTA, and the DNA was recovered by treatment with RNase A and Proteinase K, followed by phenol/chloroform and chloroform extractions and ethanol precipitation.

The DNA was digested with the restriction enzymes *Pvu*I, *Eco*RI, and *Not*I to generate a 46-bp fragment containing the radioactive repair patch, and 3 other fragments 170, 1045, and 1760 bp in length. Fragments were separated by electrophoresis through an 8% native polyacrylamide gel in 1x TBE buffer. The gel was stained for 15−30 min with a 1:20000 dilution of Sybr Green I (Molecular Probes) in electrophoresis buffer. The gel was scanned on a FluorImager SI (Molecular Dynamics) and analyzed using ImageQuant software to determine the amount of DNA per band. The fluorescent intensity of Sybr Green staining of a DNA molecular weight marker series was used to establish a standard curve for DNA quantification. The linear range is from 0.5 to 15 ng of DNA under these conditions. The gel was then dried under vacuum onto Whatman 3MM paper, transferred to a storage cassette, and allowed to expose for 2 days. The screen was scanned using a PhosphoImager 400E and analyzed for radioactive incorporation using ImageQuant software.

Radioactive incorporation per base pair per nanogram of DNA in the 46-bp band was calculated using the PhosphoImager counts with the amount of DNA determined from Sybr Green fluorescence. The 170-bp fragment was used as an internal control for nonspecific repair synthesis. The amount of incorporated radioactivity per base pair per nanogram of DNA in the 170-bp band was subtracted from the incorporated radioactivity per base pair per nanogram of DNA in the 46-bp band to yield the net damage-specific incorporation of radioactivity per base pair per nanogram of DNA. Within each experiment, the relative damage-specific incorporation for each adduct was normalized to that for the (+)-DE-1 adduct placed on G_1, which had the lowest variation among experiments.

RESULTS

Characterization of Adducted Oligonucleotides. Nonanucleotides containing a single stereospecific dG adduct derived from trans opening of BaP diol epoxides were produced by chemical synthesis and purified by HPLC; see Materials and Methods. Absolute configurations of the oligonucleotides GCT G_1G_2*T GGC containing DE-2 adducts at G_2 of *ras* codon 12 were assigned on the basis of their syntheses using phosphoramidites derived from the separated diastereomers **Si-2a** and **Si-2b**. We had previously observed (*41*) that long wavelength bands in the pyrene chromophore region (300−350 nm) of the CD spectra of oligonucleotides containing BaP DE adducts at dG are correlated with the absolute configuration of the adduct at C-10 of the hydrocarbon. Thus, dG adducted oligonucleotides that exhibit distinct, negative bands in this region were previously found upon enzymatic hydrolysis to the nucleosides to contain 10*S* adducts, whereas dG adducted oligonucleotides with positive bands contained 10*R* adducts. In the present study, the same relationship between absolute configuration and the sign of the CD band was found for the adducted oligomers synthesized stereospecifically using phosphoramidites derived from **Si-2a** and **Si-2b**. The CD spectra (Figure 3) of the modified oligonucleotides prepared in the present study unambiguously showed positive or negative bands (opposite in sign for the early- and late-eluting diastereomers) in this region. Thus, the sign of these CD bands for the adducted oligonucleotides that were formed

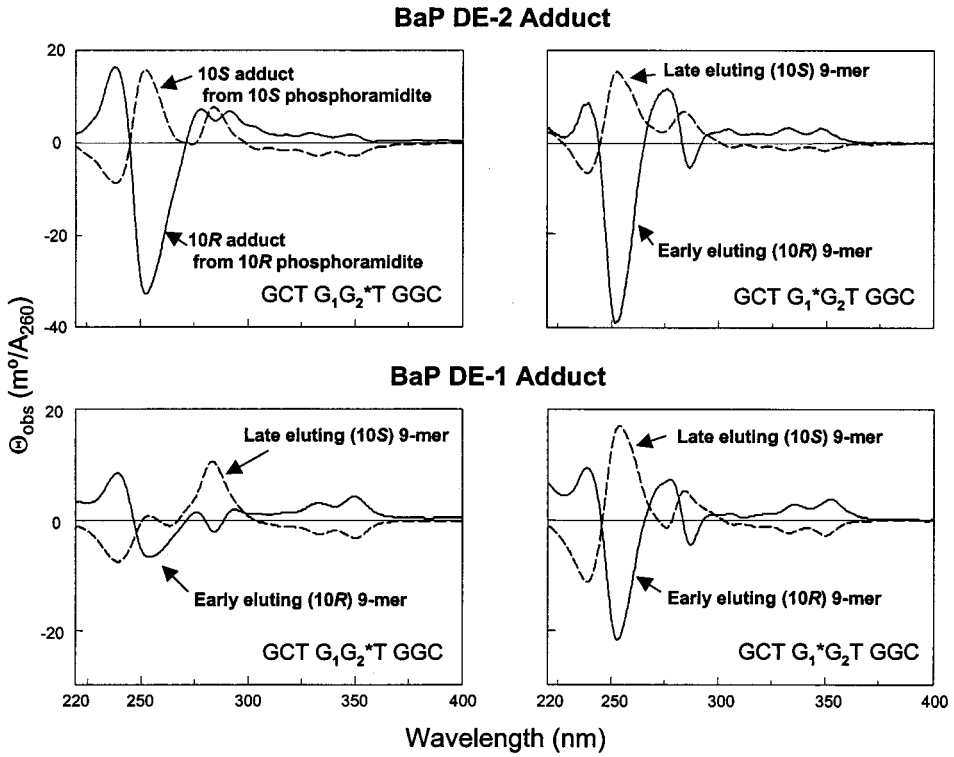

FIGURE 3: Circular dichroism spectra in aqueous solution of the modified oligonucleotide 9-mers. The asterisk indicates the position of the modified dG residue. The pair of diastereomeric oligonucleotides represented in the upper left panel were synthesized using phosphoramidites of known absolute configuration derived from the pure diastereomers **Si-2a** and **Si-2b**. For the other three pairs of diastereomeric oligonucleotides shown, absolute configuration at C-10 was assigned by comparison of their observed CD spectra with the spectra of the 9-mers of known configuration.

Table 1: Melting Temperatures and UV Shifts of 9-mers, GCT G_1G_2*T GGC, Containing trans-Opened DG Adducts at the Central G* as Duplexes with Their Complementary Strand[a]

parent DE	configuration at C-10	T_m, °C	shift[b] of pyrene absorbance on denaturation (nm)
(+)-DE-1	S	37	6
(−)-DE-1	R	40	5
(+)-DE-2	S	36	3
(−)-DE-2	R	35	2
unadducted		48	

[a] In 20 mM phosphate buffer, ionic strength 0.1 M (NaCl) at a total strand concentration of ~10 μM; see ref *47*. [b] At ~350 nm. Positive numbers represent shifts to longer wavelength upon heating the duplex from 15 to 55 °C.

by coupling with the mixed diastereomers of each phosphoramidite was used to assign their absolute configurations.

All of the 9-base oligonucleotides containing a BaP DE adduct exhibited single bands in a denaturing polyacrylamide gel that migrated more slowly than the unmodified 9-mer (*53*). The 9-mers containing trans-opened BaP DE adducts on the central G_2 were characterized by melting temperature (T_m) and spectroscopy (Table 1) of their duplexes with the complementary strand, 5′-GCC ACC AGC-3′. The oligonucleotide duplexes containing G_2 adducts exhibited a melting temperature about 10 °C lower than the unmodified duplex, with only 1−3 °C differences between the oligonucleotides containing 10*R* and 10*S* adducts derived from a given diastereomer (DE-1 or DE-2). The pyrene chromophores exhibited 2−6 nm increases in the wavelength of maximal absorbance upon melting (Table 1).

Synthesis of Single-Lesion Plasmids. Single-lesion plasmids, which contained the trans-dG adducts derived from each of the four BaP DEs placed on G_1 or G_2 of the human K-*ras* sequence, were generated using the primer extension method. The flanking 23-mer was ligated to the adducted 9-mer, with better than 90% efficiency (*53*), and the resulting 32-mer served as an efficient primer for synthesis of the second strand. The products were extensively purified by ethidium bromide/cesium chloride equilibrium centrifugation. The products were covalently closed circular plasmids with a low superhelical density and contained less than 2% nicked molecules.

Blockage of Transcription by Bacteriophage T3 RNA polymerase. Constructs containing single BaP DE adducts derived from (−)-DE-2 or (+)-DE-2, located on either G_1 or G_2, were linearized and used as templates for transcription by purified T3 RNA polymerase. Portions of the autoradiogram showing the full-length transcript (505 bases) and the blocked transcripts which stop one or two bases before the adduct site are shown in Figure 4. The adducts presented a strong but incomplete block to transcription by T3 RNA polymerase. For (+)-DE-2 adducts located on either G_1 or G_2, the blocked transcripts represent 75% of the total transcripts. For (−)-DE-2 adducts placed on G_1 or G_2, the blocked transcripts represent 83% and 75%, respectively, of the total transcripts. The proportion of blocked transcripts is essentially the same after 5 or 10 min of incubation, indicating that the production of full-length transcripts results from lesion bypass, not from repeated transcription on templates lacking a lesion.

The position of transcription blockage is subtly influenced by adduct stereochemistry and sequence. The transcript halted two bases before the adduct is more prevalent for adducts located on G_1 while the transcript halted one base before

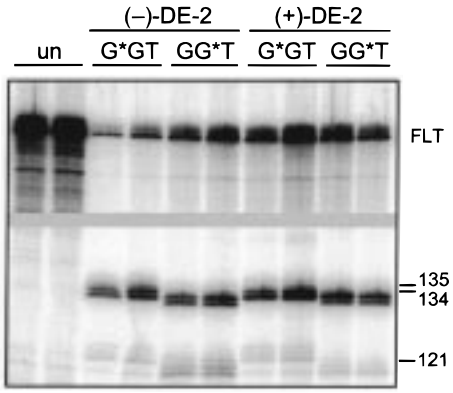

FIGURE 4: Benzo[*a*]pyrene diol epoxide adducts inhibit transcription elongation by bacteriophage T3 RNA polymerase. The paired lanes show the product after 5 or 10 min of incubation. The full-length transcript (505 bases) is shown in the upper panel, and the blocked transcript is shown in the lower panel. The intervening section of the gel is omitted. The length of the products is determined by comparison with RNA marker bands. In G*GT and GG*T constructs, the modified G is located 135 and 134 bases, respectively, from the start of transcription, while the transcripts stop one or two bases before the adduct site.

the adduct is more prevalent for adducts located on G_2. This effect is more pronounced with the (+)-DE-2 adduct than the (−)-DE-2 adduct. A minor block to transcription is also evident, producing transcripts of around 121 bases. The minor bands amount to less than 3% of the total transcripts and may result from interaction of the adducts in the template strand with the leading edge of T3 RNA polymerase.

Transcription Blockage in Nuclear Extracts. Transcription from the AdML promoter has been extensively characterized and provides for efficient transcription by RNA polymerase II with a unique point of transcript initiation (*51*). Linearized constructs containing single adducts derived from (+)- or (−)-DE-2, located on G_1 or G_2, were used as templates in an in vitro transcription reaction using human nuclear extracts. An autoradiogram of the transcription products is shown in the upper panel of Figure 5. All constructs produced a full-length transcript and bands resulting from a pause around 106 bases, while constructs containing adducts also produced blocked transcripts. An enlarged portion of the autoradiogram containing the blocked transcripts is shown in the lower panel. For the adducts derived from (−)-DE-2 located on either G_1 or G_2, as well as for adducts derived from (+)-DE-2 located on G_1, the major blockage of transcription occurred after incorporation of the base opposite the adducted base, whereas for the adduct derived from (+)-DE-2 placed on G_2, the major blockage of transcription occurred one base before the adducted base. For all of these constructs, some bypass of the lesion occurred to produce a full-length transcript. The fraction of total transcript blocked at the adduct site was quantified and revealed that each of the isomers blocked RNA polymerase II elongation by 45−50%.

Repair by Human Whole Cell Extract. The single-lesion plasmids were used as substrates in DNA repair synthesis assays using whole cell extracts derived from a normal human lymphoblastoid cell line. As shown in Figure 6, the Sybr Green I fluorescence shows approximately equal loading of the DNA in all lanes. Damage-specific incorporation of radioactivity representing DNA repair synthesis is evident in the 46-bp fragment compared with the unmodified

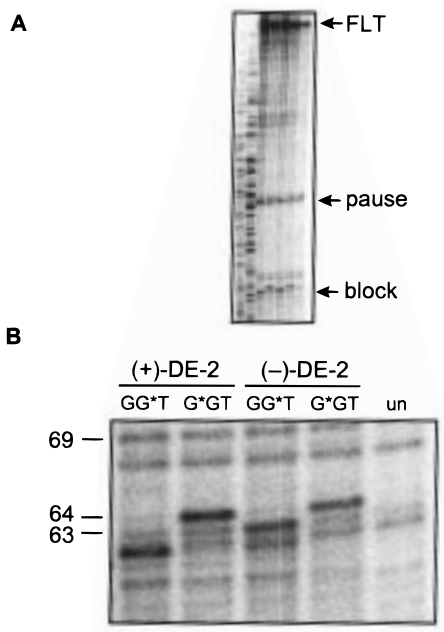

FIGURE 5: Blockage of human RNA polymerase II transcription by templates containing adducts derived from benzo[*a*]pyrene (+)-DE-2 or (−)DE-2 or without an adduct. (A) Autoradiogram of transcription products. Two picomoles of linearized template were incubated with 70 μg of nuclear extract protein at 30 °C for 60 min. The full-length transcript (FLT) is 434 bases, and the bands marked "pause" are 105−108 bases in length. (B) Enlarged section of autoradiogram showing blocked transcripts. The adducts placed on G*GT are located 64 bases from the start of transcription, and the adducts placed on GG*T are located 63 bases from the start of transcription. The bands at 67 and 69 bases correspond to pause sites found in modified and unmodified templates. The positions of RNA marker bands of the indicated sizes are shown.

control. The incorporation of radioactivity into the 46-bp band was corrected for background incorporation as described in the Experimental Procedures. Damage-specific DNA repair synthesis was measured after 90 min of incubation, normalized to the value for the (+)-DE-1 adduct on G_1, and displayed in Figure 6 as a histogram. Adducts derived from a given stereoisomer exhibited little difference whether placed on G_1 or G_2. On the basis of average of the two positions, the trend in repair efficiency decreased in the following order: (+)-DE-2 ≈ (−)-DE-1 > (+)-DE-1 ≫ (−)-DE-2, although differences among the first three are not statistically significant. The extent of repair of adducts derived from (−)-DE-2 is significantly lower than that of the corresponding (+)-DE-2 adduct at either the G_1 or G_2 location ($p < 0.002$ and $p < 0.017$, respectively, based on Student's t test.) The specific incorporation of radioactivity for the (−)-DE-2 constructs is not significantly different from the incorporation into the analogously prepared unmodified construct.

The 46-bp fragments containing the adducts have identical electrophoretic mobilities, except for the fragment derived from the construct containing (+)-DE-2 adducts on G_2, which shows a second, more intense, slower-moving band in the Sybr Green I-stained gel (Figure 6A, upper part). Radioactivity due to repair synthesis (Figure 6A, lower part) only appears in a single 46-bp band. The two Sybr Green I bands do not correspond to an unrepaired, adducted 46-mer and a repaired, no longer adducted 46-mer, because the overall extent of repair is too small to produce a distinct Sybr Green

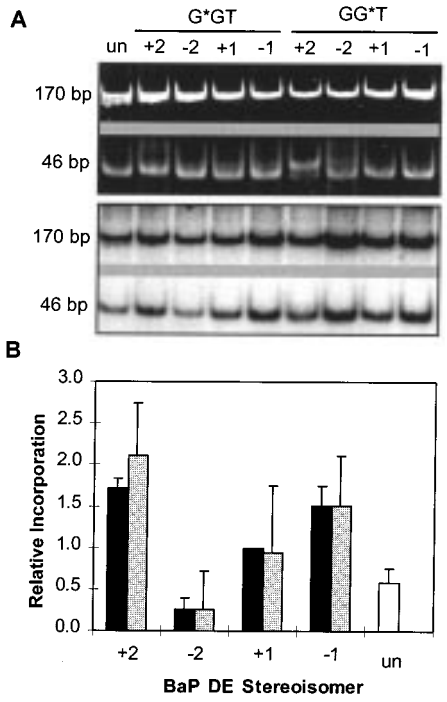

FIGURE 6: DNA repair synthesis by human whole cell extracts in plasmids containing single benzo[*a*]pyrene diol epoxide adducts. The numeric designations refer to constructs containing adducts derived from the corresponding diol epoxides; for example, +2 is derived from (+)-DE-2. Reactions contained 100 μg of WCE and 100 ng of single-lesion plasmid and were incubated at 30 °C for 90 min. (A) Portions of gel images showing DNA loading and incorporation of radioactivity into specific and nonspecific fragments. The upper panels show the Sybr Green I-stained fluorescence of the 170-bp band and the 46-bp band. The 46-bp band, generally in the amounts of 1−3 ng, was used to determine the amount of DNA loaded in comparison with DNA standards. The lower panels show the incorporation of radioactivity into the 170- and 46-bp bands. (B) The relative, damage-specific incorporation of radioactivity for each adduct was determined by subtracting length-adjusted nonspecific incorporation per nanogram of DNA determined from the 170-bp band from the length-adjusted incorporation per nanogram of DNA into the 46-bp band, and normalizing to the specific incorporation for the adduct derived from (+)-DE-1 placed on G_1. The black bars represent the relative incorporation for adducts located on G_1, and the gray bars represent the relative incorporation for adducts located on G_2. The white bar represents the incorporation into the unmodified control construct. Values given are the mean and standard deviation of three experiments.

I fluorescent band of the intensity seen. Furthermore, a variable amount of the faster-moving band is produced from the single-lesion plasmid containing the (+)-DE-2 adduct at G_2 by a mock treatment in which the cell extract is omitted. We interpret the existence of two bands with distinct mobilities as indicating the existence of at least two conformations of the (+)-DE-2 adduct, as suggested previously (*15, 23, 55*). A stereospecific increase in flexibility of DNA fragments containing trans-opened (+)-DE-2 adducts at dG, with a resulting decrease in gel mobility, has been observed for the sequence TG*T (*56, 57*).

The extensive amount of DNA repair synthesis incurred in the remainder of the plasmid is a characteristic of DNA constructs made in this manner (*58*−*60*). The high level of background synthesis does not interfere with the determination of repair for lesions recognized well by the NER system, but for poorly repaired lesions, specific incorporation is barely above background (*58*). Although the set of 8 single-lesion constructs used in this study was prepared by the same method, the level of nonspecific repair synthesis varies considerably from one construct to another. These differences may result from relatively minor differences in handling.

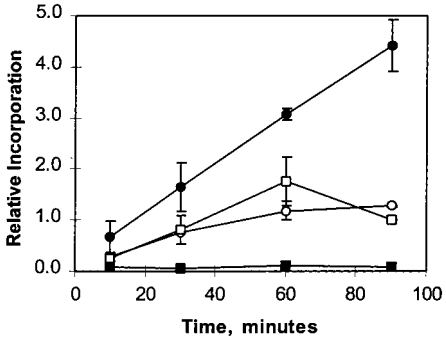

FIGURE 7: Time course of damage-specific incorporation for adducts placed on G1. Reactions contained 100 μg of normal human WCE and were incubated at 30 °C for 10−90 min. Damage-specific incorporation into the 46-bp fragment was normalized to the value at 90 min for the (+)-DE-2 construct. Data are expressed as the mean and standard deviation of two experiments. The symbols used are the following: open squares, (+)-DE-2; filled squares, (−)-DE-2; open circles, (+)-DE-1; filled circles, (−)-DE-1.

The time course of repair for adducts placed on G_1 was determined, and the averaged results from two trials are shown in Figure 7. For three of the four constructs, damage-specific incorporation increased over 90 min without reaching a plateau. The level of repair synthesis in constructs containing the adduct derived from (+)-DE-2 reached a maximum level around 60 min and decreased somewhat with further incubation to 90 min. The levels of repair incorporation observed after 90 min of incubation are similar to the results shown in Figure 6 for three of the four constructs. Curiously, the results for the construct containing the (−)-DE-1 adduct differ considerably between the two sets of experiments (see below). The time course of repair incorporation for adducts placed on G_2 was investigated in a single experiment (data not shown). The damage-specific incorporation generally increased with incubation time, and the levels of incorporation at 90 min are similar to those shown in Figure 6.

In the first set of experiments (shown in Figure 6), the repair incorporation for the (−)-DE-1 constructs, following 90 min of incubation, was slightly less than the incorporation into the (+)-DE-2 constructs, whereas in the second set of experiments (shown in Figure 7), the incorporation into the (−)-DE-1 constructs was 3−4 times greater than the incorporation into the (+)-DE-2 construct. This change in the amount of repair label incorporated into the (−)-DE-1 construct was not accompanied by a change in the fraction of nicked molecules or in the mobility of the fragment containing the adduct. This change in behavior could not be attributed to a difference in the handling or storage of the constructs.

Nicked Construct Extent of Repair. Within this sequence, the greatest difference in the extent of repair was observed between the (+)-DE-2 and (−)-DE-2 adducts. To investigate the possibility that the low rate of repair of the (−)-DE-2 adduct was due to a specific inhibition of the 3′ -incision, we generated nicked constructs for both (+)-DE-2 and (−)-DE-2 adducts placed on G_1 and an unmodified control. These constructs contained a nick at the sixth phosphodiester bond

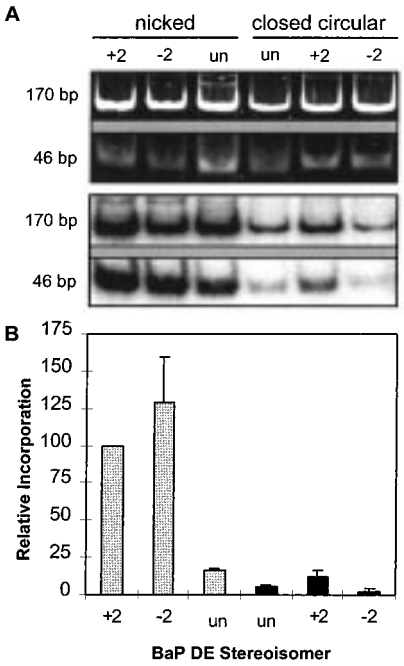

FIGURE 8: Repair of (+)-DE-2 and (−)-DE-2 adducts placed on G_1 in covalently closed circles or in nicked constructs. (A) Gel images. The upper panel shows the Sybr Green I-stained gel, indicating the loading of the DNA, and the lower panel shows the incorporation of radioactivity. The 46-bp band contains the repair patch, and the 170-bp band is an adjacent fragment without specific damage. (B) The specific incorporation in the 46-bp band has been normalized to the incorporation of the nicked construct containing the (+)-DE-2 adduct and represents the mean of two experiments. The gray bars represent the nicked constructs, and the black bars represent the covalently closed circular constructs. Note that the order of the samples differs in the two series.

3′ to the adduct. Repair synthesis assays were performed. The damage-specific incorporation was about 9-fold greater in the nicked construct containing the (+)-DE-2 adduct compared with the corresponding covalently closed circular construct (Figure 8). The extent of repair was similar for the nicked constructs containing (+)-DE-2 and (−)-DE-2 adducts, in contrast to the defect in repair for the (−)-DE-2 adduct located in covalently closed circular plasmid. Background nonspecific repair synthesis also increased but only by approximately 3-fold. The increase in nonspecific DNA synthesis is expected in the nicked constructs because molecules containing randomly located nicks are not removed during purification.

DISCUSSION

Synthesis of dG Adducted Oligonucleotides. Although site-specific modification of dG residues in oligonucleotides by BaP DEs is of considerable interest, since the major DNA lesion produced from BaP in vivo is a trans-opened dG DE-2 adduct, methods for preparation of oligonucleotides with BaP DE adducts at dG have largely been limited to direct alkylation of oligonucleotides (*61*), preferably containing a single dG residue, by the appropriate diol epoxide, followed by chromatographic separation of the heterogeneous products obtained. The lack of specificity of the direct alkylation method makes it particularly unsuitable for site-specific modification of biologically interesting purine-rich sequences such as the human K-*ras* sequence, which contains five dG residues that are potential targets for the diol epoxide. We have chosen the approach of synthesizing BaP DE adducts at N^2 of dG as protected phosphoramidites suitable for incorporation into any desired oligonucleotide sequence by standard solid-phase synthesis. Generation of a protected diol epoxide adduct by coupling of the amino triacetate derived from trans opening of BaP DE-2 with an O^6-protected di-*O*-TBDMS 2-trifluoromethanesulfonyl derivative of deoxyinosine has been reported in 5% yield (*62*). Use of the unprotected aminotriol and a fluoride rather than a trifluoromethanesulfonate leaving group on deoxyinosine (see Scheme 1) gave yields of 40−60% for this critical, adduct-forming step. The present method is parallel to that which we have previously used (*47*) for the synthesis of adducted dA phosphoramidites. To our knowledge this represents the first practical route for the synthesis of trans-opened N^2-dG adducts as protected phosphoramidites for oligonucleotide synthesis. We have successfully employed these phosphoramidites for solid-phase synthesis of six of the eight *ras* 9-mers utilized in the present study. An alternative approach, postoligomerization reaction (*49*) of a support-bound 9-mer containing a 2-fluorodeoxyinosine residue with a BaP aminotriol, was used for synthesis of the remaining two modified oligonucleotides.

Groove-Bound Conformations of trans-Ring-Opened dG Adducts. For adducts of a given diastereomer (DE-1 or DE-2) the difference in T_m (Table 1) between the modified oligonucleotide duplexes with 10*R* and 10*S* absolute configurations at the point of attachment of the hydrocarbon to N^2 of dG is small (1−3 °C). These differences are similar to those for oligonucleotides containing trans-opened dG adducts in another sequence context (*63*) in which the hydrocarbon portion of DE-2 is known (*18, 19*) to lie in the minor groove. In contrast, oligonucleotide duplexes containing intercalated BaP N^6-dA adducts (*17, 64*) exhibit significantly lower (∼8−12 °C for 9- and 11-mers) T_m values for adducts with 10*S* compared to 10*R* absolute configuration. Shifts of λ_{max} for the pyrene bands at 300−360 nm to longer wavelengths on denaturation correspond to shifts to shorter wavelength on duplex formation (15 °C) from the separated strands (55 °C). The direction of these shifts suggests that there is less stacking between the pyrene chromophore and the bases in the duplexes than in the denatured, single strands, and is consistent with a groove-bound (nonintercalated) orientation of the hydrocarbons in the adducted duplexes.

Blockage of Transcription by BaP Adducts. An immediate cellular effect of DNA damage is interference with transcription. We have examined the effect of stereospecific BaP adducts on transcription elongation either by purified bacteriophage T3 RNA polymerase or by human RNA polymerase II in the context of a nuclear extract. We observed that the BaP adducts present a strong but not complete block to T3 RNA polymerase transcription elongation, with little difference in the degree of bypass exhibited between the stereoisomers. This contrasts with inhibition of transcription by bacteriophage T7 RNA polymerase by BaP adducts in a CG*C context, in which (+)-DE-2 adducts inhibited transcription more completely than (−)-DE-2 adducts (*65, 66*). In addition, transcription by T3 RNA polymerase is halted one or two bases before the adducted base (see results), while transcription by T7 RNA polymerase halts after addition of a ribonucleotide across from the adducted base (*66*). In contrast to the results with purified bacteriophage RNA

polymerases, the (+)- and (−)-DE-2 adducts present an intermediate blockage to RNA polymerase II transcription elongation in the presence of nuclear extract. Transcription bypass of these minor groove-located adducts may be facilitated by elongation factors such as SII (*67*).

Stereospecific Differences in Repair of BaP Adducts. In the present study, we examined the repair by human cell extracts of the trans dG adducts derived from (+)- and (−)-DE-2 and (+)- and (−)-DE-1. These adducts were placed in the immediate sequence context of TG*G (G_1 adducts) or GG*T (G_2 adducts). The greatest difference in the extent of repair was observed between the (+)-DE-2 and (−)-DE-2 adducts. The constructs containing the (−)-DE-2 adducts experienced levels of DNA repair synthesis not significantly different from that of the unmodified construct. Interestingly, the (−)-DE-2 trans adducted N^2-dG was also poorly repaired by the *Escherichia coli* UvrABC excision repair system (*68*). The pyrenyl rings of the trans (−)-DE-2 adduct are pointed toward the 3′-end of the adducted strand whereas the pyrenyl rings of the trans (+)-DE-2 adduct are pointed toward the 5′-end of the adducted strand (*18*, *19*). The human NER enzymes incise the DNA 5−7 nucleotides 3′ to the damaged base and 22−24 nucleotides to the 5′ (*69*). The pyrenyl rings extend at most only two nucleotides from the adducted base and do not physically obstruct the 3′ incision. Thus the difference in the repair of the (+)- and (−)-DE-2 adducts must be the result of an indirect effect, possibly by preventing DNA−protein contacts necessary for the assembly of the repair complex or because the (−)-DE-2 adduct causes only minor perturbations in the helix structure and is poorly recognized by the NER proteins. The (+)-DE-2 adduct, but not the (−)-DE-2 adduct, is associated with an increase in helix bending and flexibility for adducts located in the sequence TG*T (*57*). In the sequence CG*C, the groove-bound, trans-opened adducts derived from (+)- and (−)-DE-2 were repaired by human cell extracts at one tenth the rate of the intercalated, cis-opened adducts (*70*). No significant difference in repair was reported between the trans (+)-DE-2 and trans (−)-DE-2 adducts (*70*).

The increased damage-specific repair synthesis for both the (+)-DE-2 and (−)-DE-2 nicked constructs may reflect increased recognition due to the combined effects of the nick and the adduct on the DNA helix structure. One possible explanation for the low level of repair of the (−)-DE-2 adduct in the covalently closed circular construct is that the 3′ orientation of the pyrene rings specifically inhibited the 3′ incision during NER. The observed large increase in DNA repair synthesis for both the (+)-DE-2 and (−)-DE-2 constructs precludes attributing the increase in repair to relief of a putatively inhibited 3′ incision and suggests rather that increases in helix distortion and flexibility may increase recognition. It would be interesting to see if a nick placed near the adducts on the 5′ side similarly increased the rate of repair. Another interpretation of the increase in damage-specific incorporation in the pre-nicked construct compared with the covalently closed construct is that presence of an adduct near the nick provides for greater incorporation of radioactivity without specifically increasing the extent of NER. The involvement of this mechanism requires a looping out of the adducted and adjacent bases with misaligned annealing of the remaining bases to provide a primer for DNA synthesis without repair. Such an event is possible in the present system because of the repeated sequence TG*GTGG surrounding the adduct. The presence of a nick immediately 3′ or 5′ to a bulky lesion decreased but did not abolish incision by *Escherichia coli* UvrABC enzymes (*71*).

Sequence Specificity of Repair. Although no differences between adducts located on the two guanines within the sequence TG_1G_2T were detected in the present work, others have reported sequence-dependent differences in repair rates. In human fibroblasts, site-specific rates of repair of BaP DE adducts in the hypoxanthine phophoribosyltransferase (HPRT) gene varied by more than a factor of 10 (*72*). In the human p53 gene, many sites of slow repair of cyclobutane dimers correspond to mutation hot spots (*32*). The extent of excision of AAF adducts located on each of the guanines in the sequence GGCGCC varied by a factor of 3 in experiments using HeLa WCE (*73*). The recognition of adducts by the DNA repair system as well as the competing processes of binding of transcription factors or other proteins ultimately may be determined by adduct DNA conformation, which is controlled by both specific adduct stereochemistry and by local DNA structure.

Overall Repair Efficiency and Relation to Transcription Coupled Repair. Damage recognition by the mammalian NER system varies widely for different adduct types. The intercalated, helix-distorting AAF-dG adducts are recognized 40-fold more efficiently than the groove-bound BaP DE trans-dG adducts (*59*). The cis-opened dG adducts formed from (+)- and (−)-DE-2, which intercalate and distort the helix, are repaired more efficiently than trans-opened dG adducts (*70*). On the basis of in vitro DNA repair assays, the recognition efficiency of the NER system for various adducts may be placed in the following order: AAF > (6−4) photoproduct ≅ BaP DE *cis*-dG > cyclobutane dimer > BaP DE trans-dG > 8-methoxypsoralen > anthramycin > CC-1065 (*58*, *70*, *74*, *75*). BaP adducts in cells and tissues are removed slowly and persist with a half-life of 3−4 days (*76*−*79*). We have shown that trans-dG adducts of BaP are poorly repaired in vitro, in agreement with earlier work, but the defect in the repair of (−)-DE-2 adducts in the present system is novel and may relate to the persistence of BaP adducts.

The strand bias in the mutation spectra produced by BaP suggests that adducts are removed more rapidly from the transcribed strand of active genes by transcription coupled repair (TCR) (*34*, *35*). Moreover, the strand bias for mutations formed from (−)-DE-2 is nearly as distinct as that produced by (+)-DE-2 (*36*). We have shown that BaP adducts are strong blocks to transcription elongation by bacteriophage T3 RNA polymerase, which is similar to previously described results with bacteriophage T7 RNA polymerase (*66*). However, we have also shown that both (+)- and (−)-DE-2 BaP adducts are only weak blocks to RNA polymerase II in experiments using HeLa nuclear extracts. The blockage of transcription by RNA polymerase II is generally considered to be an early important event in TCR. The absence of a strong block to RNA polymerase II transcription elongation by the BaP adducts suggests that lesion bypass can occur under some circumstances and may relate to the conflict in reports of TCR of BaP lesions in vivo (*37*, *38*).

SUMMARY

We have presented methods for the chemical synthesis and purification of oligonucleotides containing stereospecific dG adducts derived from trans opening of benzo[*a*]pyrene diol epoxides at defined sites in an oligonucleotide. These adducts were placed within the G-rich sequence corresponding to a mutation hot spot located at codon 12 in the human K-*ras* sequence, and the effects of the adducts on transcription and DNA repair were examined by in vitro assays. With a human enzyme system, no differences were observed in the repair of adducts located on the first or second G of the codon 12 sequence, GGT, but there was a significant stereospecific difference in the extent of repair between the adducts derived from (+)-DE-2 (significant repair) and (−)-DE-2 (no significant repair). The adducts present strong blocks to transcription elongation by purified T3 RNA polymerase, but only weakly block transcription by RNA polymerase II in nuclear extracts derived from HeLa cells. These results and others (*70*) indicate that there are differences between the individual stereoisomers of benzo[*a*]-pyrene diol epoxide adducts as well as effects of surrounding sequence in the processing of these lesions.

ACKNOWLEDGMENT

The authors express appreciation to D. Reines (Emory U.) for providing the AdML promoter plasmid and to N. Hoehr, R. Selzer, and R. Stierum for critically reading the manuscript.

SUPPORTING INFORMATION AVAILABLE

Three tables providing details of chromatographic separation of diastereomers **Si-1a/b** and **Si-2a/b**, ^{1}H NMR and mass spectra for **Si-1a/b**, **Si-2a/b**, **DMT-1a/b**, and **DMT-2a/b,** and HPLC conditions for the purification of adducted oligonucleotides (5 pages). Ordering information is given on any current masthead page.

REFERENCES

1. Pitot, H. C. (1993) *Cancer 72*, 962−970.
2. Ziegler, D. M. (1991) *Drug. Metab. Dispos. 19*, 847−852.
3. Thakker, D., Yagi, H., Levin, W., Wood, A., Conney, A., and Jerina, D. (1985) in *Bioactivation of Foreign Compounds* (Anders, M. W., Ed.) pp 177−242, Academic Press, Orlando, FL.
4. Jerina, D. M., Lehr, R. E., Yagi, H., Hernandez, O., Dansette, P. M., Wislocki, P. G., Wood, A. W., Chang, R. L., Levin, W., and Conney, A. H. (1976) in *In Vitro Metabolic Activation in Mutagenesis Testing* (de Serres, F. J., Fouts, J. R., Bend, J. R., and Philpot, R. M., Eds.) pp 159−177, Elsevier/North-Holland Biomedical Press, Amsterdam, The Netherlands.
5. Jerina, D. M., and Lehr, R. E. (1977) in *Microsomes and Drug Oxidations: 3rd International Symposium* (Ullrich, V., Roots, I., Hildebrandt, A. G., Estabrook, R. W., and Conney, A. H., Eds.) pp 709−723, Pergamon Press, Oxford, England.
6. Jerina, D. M., Yagi, H., Thakker, D. R., Sayer, J. M., van Bladeren, P. J., Lehr, R. E., Whalen, D. L., Levin, W., Chang, R. L., Wood, A. W., and Conney, A. H. (1984) in *Foreign Compound Metabolism* (Caldwell, J., and Paulson, G. D., Eds.) pp 257−266, Taylor and Francis, Ltd., London, U.K.
7. Thakker, D. H., Yagi, H., Akagi, H., Koreeda, M., Lu, A. Y. H., Levin, W., Wood, A. W., Conney, A. H., and Jerina, D. M. (1977) *Chem.-Biol. Interact. 16*, 281−300.
8. Buening, M. K., Wislocki, P. G., Levin, W., Yagi, H., Thakker, D. R., Akagi, H., Koreeda, M., Jerina, D. M., and Conney, A. H. (1978) *Proc. Natl. Acad. Sci. U.S.A. 75*, 5358−5361.
9. Jerina, D. M., Chadha, A., Cheh, A. M., Schurdak, M. E., Wood, A. W., and Sayer, J. M. (1991) in *Biological Reactive Intermediates IV* (Witmer, C. M., Snyder, R., Jollow, D. J., Kalf, G. F., Kocsis, J. J., and Sipes, I. G., Eds.) pp 533−553, Plenum Press, New York.
10. Cheng, S. C., Hilton, B. D., Roman, J. M., and Dipple, A. (1989) *Chem. Res. Toxicol. 2*, 334−340.
11. Sayer, J. M., Chadha, A., Agarwal, S. K., Yeh, H. J. C., Yagi, H., and Jerina, D. M. (1991) *J. Org. Chem. 56*, 20−29.
12. Jerina, D. M., Sayer, J. M., Yeh, H. J. C., Liu, X., Yagi, H., Schurter, E., and Gorenstein, D. (1996) *Polycyclic Aromat. Compd. 10*, 145−152.
13. Geacintov, N. E., Cosman, M., Hingerty, B. E., Amin, S., Broyde, S., and Patel, D. J. (1997) *Chem. Res. Toxicol. 10*, 111−146.
14. Geacintov, N., Cosman, M., Mao, B., Alfano, A., Ibanez, V., and Harvey, R. (1991) *Carcinogenesis 12*, 2099−2108.
15. Zhao, R., Liu, T.-M., Kim, S. K., MacLeod, M. C., and Geacintov, N. E. (1992) *Carcinogenesis 13*, 1817−1824.
16. Yeh, H. J. C., Sayer, J. M., Liu, X., Altieri, A. S., Byrd, R. A., Lakshman, M. K., Yagi, H., Schurter, E. J., Gorenstein, D. G., and Jerina, D. M. (1995) *Biochemistry 34*, 13570−13581.
17. Schurter, E. J., Yeh, H. J. C., Sayer, J. M., Lakshman, M. K., Yagi, H., Jerina, D. M., and Gorenstein, D. G. (1995) *Biochemistry 34*, 1364−1375.
18. Cosman, M., de los Santos, C., Fiala, R., Hingerty, B. E., Singh, S. B., Ibanez, V., Margulis, L. A., Live, D., Geacintov, N. E., Broyde, S., and Patel, D. J. (1992) *Proc. Natl. Acad. Sci. U.S.A. 89*, 1914−1918.
19. de los Santos, C., Cosman, M., Hingerty, B. E., Ibanez, V., Margulis, L. A., Geacintov, N. E., Broyde, S., and Patel, D. J. (1992) *Biochemistry 31*, 5245−5252.
20. Cosman, M., de los Santos, C., Fiala, R., Hingerty, B. E., Ibanez, V., Luna, E., Harvey, R., Geacintov, N. E., Broyde, S., and Patel, D. J. (1993) *Biochemistry 32*, 4145−4155.
21. Cosman, M., Hingerty, B. E., Luneva, N., Amin, S., Geacintov, N. E., Broyde, S., and Patel, D. J. (1996) *Biochemistry 35*, 9850−9863.
22. Suh, M., Jankowiak, R., Ariese, F., Mao, B., Geacintov, N. E., and Small, G. J. (1994) *Carcinogenesis 15*, 2891−2898.
23. Fountain, M. A., and Krugh, T. R. (1995) *Biochemistry 34*, 3152−3161.
24. Zhu, D., Keohavong, P., Finkelstein, S. D., Swalsky, P., Bakker, A., Weissfeld, J., Srivastava, S., and Whiteside, T. L. (1997) *Cancer Res. 57*, 2485−2492.
25. Gao, H.-G., Chen, J.-K., Stewart, J., Song, B., Rayappa, C., Whong, W.-Z., and Ong, T. (1997) *Carcinogenesis 18*, 473−478.
26. Lacal, J. C. (1997) *FEBS Lett. 410*, 73−77.
27. Dittrich, K., and Krugh, T. (1991) *Chem. Res. Toxicol. 4*, 277−281.
28. Denissenko, M. F., Pao, A., Tang, M.-s., and Pfeifer, G. P. (1996) *Science 274*, 430−432.
29. Bohr, V. A., Smith, C. A., Okumoto, D. S., and Hanawalt, P. C. (1985) *Cell 40*, 359−369.
30. Mellon, I., Spivak, G., and Hanawalt, P. C. (1987) *Cell 51*, 241−249.
31. Evans, M. K., Taffe, B., Harris, C. C., and Bohr, V. A. (1993) *Cancer Res. 53*, 5377−5381.
32. Tornaletti, S., and Pfeifer, G. P. (1994) *Science 263*, 1436−1438.
33. Gao, S., Drouin, R., and Holmquist, G. P. (1994) *Science 263*, 1438−1440.
34. Chen, R.-H., Maher, V. M., and McCormick, J. J. (1990) *Proc. Natl. Acad. Sci. U.S.A. 87*, 8680−8684.
35. Wei, S.-J. C., Chang, R. L., Bhachech, N., Cui, X. X., Merkler, K. A., Wong, C.-Q., Hennig, E., Yagi, H., Jerina, D. M., and Conney, A. H. (1993) *Cancer Res. 53*, 3294−3301.
36. Wei, S.-J. C., Chang, R. L., Hennig, E., Cui, X. X., Merkler, K. A., Wong, C.-Q., Yagi, H., Jerina, D. M., and Conney, A. H. (1994) *Carcinogenesis 15*, 1729−1735.

37. Chen, R.-H., Maher, V. M., Brouwer, J., van de Putte, P., and McCormick, J. J. (1992) *Proc. Natl. Acad. Sci. U.S.A. 89*, 5413−5417.
38. Tang, M.-s., Pao, A., and Zhang, X.-s. (1994) *J. Biol. Chem. 269*, 12749−12754.
39. Carothers, A. M., Zhen, W., Mucha, J., Zhang, Y.-J., Santella, R. M., Grunberger, D., and Bohr, V. A. (1992) *Proc. Natl. Acad. Sci. U.S.A. 89*, 11925−11929.
40. Sambrook, J., Fritsch, E., and Maniatis, T. (1989) *Molecular Cloning: A Laboratory Manual*, Cold Spring Harbor Press, Cold Spring Harbor, NY.
41. Page, J. E., Zajc, B., Oh-hara, T., Lakshman, M. K., Sayer, J. M., Jerina, D. M., and Dipple, A. (1998) *Biochemistry 37*, 9127−9137.
42. Lakshman, M. K., Sayer, J. M., and Jerina, D. M. (1991) *J. Am. Chem. Soc. 113*, 6589−6594.
43. Yagi, H., Thakker, D. R., Hernandez, O., Koreeda, M., and Jerina, D. M. (1977) *J. Am. Chem. Soc. 99*, 1604−1611.
44. Zajc, B., Lakshman, M. K., Sayer, J. M., and Jerina, D. M. (1992) *Tetrahedron Lett. 33*, 3409−3412.
45. Moore, P. D., Koreeda, M., Wislocki, P. G., Levin, W., Conney, A. H., Yagi, H., and Jerina, D. M. (1977) in *Drug Metabolism Concepts* (Jerina, D. M., Ed.) American Chemical Society, Washington, DC.
46. Nicolaou, K. C., and Webber, S. E. (1986) *Synthesis*, 453−461.
47. Lakshman, M. K., Sayer, J. M., Yagi, H., and Jerina, D. M. (1992) *J. Org. Chem. 57*, 4585−4590.
48. Beaucage, S. L. (1993) in *Methods in Molecular Biology* (Agrawal, S., Ed.) pp 33−61, Humana Press, Totowa, NJ.
49. Harris, C. M., Zhou, L., Strand, E. A., and Harris, T. M. (1991) *J. Am. Chem. Soc. 113*, 4328−4329.
50. Christner, D. F., Lakshman, M. K., Sayer, J. M., Jerina, D. M., and Dipple, A. (1994) *Biochemistry 33*, 14297−14305.
51. Aso, T., Conway, J. W., and Conway, R. C. (1994) *J. Biol. Chem. 269*, 26575−26583.
52. Wood, R. D., Biggerstaff, M., and Shivji, M. K. K. (1995) *Methods: A Companion to Methods Enzymol. 7*, 163−175.
53. Custer, L. (1997) Ph.D. Dissertation, American University, Washington, DC.
54. Dignam, J. D., Lebovitz, R. M., and Roeder, R. G. (1983) *Nucleic Acids Res. 11*, 1475−1489.
55. Kozack, R. E., and Loechler, E. L. (1997) *Carcinogenesis 18*, 1585−1593.
56. Xu, R., Mao, B., Xu, J., Li, B., Birke, S., Swenberg, C. E., and Geacintov, N. E. (1995) *Nucleic Acids Res. 23*, 2314−2319.
57. Xu, R., Mao, B., Amin, S., and Geacintov, N. E. (1998) *Biochemistry 37*, 769−778.
58. Szymkowski, D. E., Lawrence, C. W., and Wood, R. D. (1993) *Proc. Natl. Acad. Sci. U.S.A. 90*, 9823−9827.
59. Hess, M. T., Gunz, D., and Naegli, H. (1996) *Nucleic Acids Res. 24*, 824−828.
60. Moggs, J. G., Yarema, K. J., Essigmann, J. M., and Wood, R. D. (1996) *J. Biol. Chem. 271*, 7177−7186.
61. Cosman, M., Ibanez, V., Geacintov, N. E., and Harvey, R. G. (1990) *Carcinogenesis 11*, 1667−1672.
62. Steinbrecher, T., Wameling, V. C., Oesch, F., and Seidel, A. (1993) *Angew. Chem., Int. Ed. Engl. 32*, 404−406.
63. Ya, N.-Q., Smirnov, S., Cosman, M., Bhanot, S., Ibanez, V., and Geacintov, N. E. (1994) in *Structural Biology: The State of the Art, Proceedings of the Eighth Conversation* (Sarma, R. H., and Sarma, M. H., Eds.) pp 349−366, Adenine Press, Schenactady, NY.
64. Schurter, E. J., Sayer, J. M., Oh-hara, T., Yeh, H. J. C., Yagi, H., Luxon, B. A., Jerina, D. M., and Gorenstein, D. G. (1995) *Biochemistry 34*, 9009−9020.
65. Choi, D.-J., Marino-Alessandri, D. J., Geacintov, N. E., and Scicchitano, D. A. (1994) *Biochemistry 33*, 780−787.
66. Choi, D.-J., Roth, R. B., Liu, T., Geacintov, N. E., and Scicchitano, D. A. (1996) *J. Mol. Biol.*, 213−219.
67. Mote, J., Jr., Ghanouni, P., and Reines, D. (1994) *J. Mol. Biol. 236*, 725−737.
68. Zou, Y., Liu, T.-M., Geacintov, N. E., and Van Houten, B. (1995) *Biochemistry 34*, 13582−13593.
69. Sancar, A. (1996) *Annu. Rev. Biochem. 65*, 1436−1438.
70. Hess, M. T., Gunz, D., Luneva, N., Geacintov, N. E., and Naegli, H. (1997) *Mol. Cell. Biol. 17*, 7069−7076.
71. Snowden, A., Kow, Y. W., and Van Houten, B. (1990) *Biochemistry 29*, 7251−7259.
72. Wei, D., Maher, V. M., and McCormick, J. J. (1995) *Proc. Natl. Acad. Sci. U.S.A. 92*, 2204−2208.
73. Mu, D., Bertrand-Burggraf, E., Huang, J.-C., Fuchs, R. P. P., and Sancar, A. (1994) *Nucleic Acids Res. 22*, 4869−4871.
74. Hansson, J., and Wood, R. D. (1989) *Nucleic Acids Res. 17*, 8073−8079.
75. Gunz, D., Hess, M. T., and Naegli, H. (1996) *J. Biol. Chem. 271*, 25089−25098.
76. Celotti, L., Ferraro, P., Furlan, D., Zanesi, N., and Pavanello, S. (1993) *Proc. Natl. Acad. Sci. U.S.A. 91*, 12213−12217.
77. Stierum, R., Van Wolterbeek, A., Melis, O., Wittekoek, M., Rutten, A., Feron, V., and Baan, R. (1994) *Mutat. Res. 325*, 31−37.
78. Roggeband, R., Wolterbeek, A. P. M., Melis, O. W. M., Wittekoek, M. E., Rutten, A. A. J. J. L., Feron, V. J., and Baan, R. A. (1994) *Carcinogenesis 15*, 661−665.
79. Suh, M., Ariese, F., Small, G. J., Jankowiak, R., Hewer, A., and Phillips, D. H. (1995) *Carcinogenesis 16*, 2561−2569.

BI9813330